

Title	Constraining magnetization of gamma-ray bursts outflows using prompt emission fluence
Author(s)	Pe'er, Asaf
Publication date	2017
Original citation	Asaf, P. (2017) 'Constraining magnetization of gamma-ray bursts outflows using prompt emission fluence', <i>Astrophysical Journal</i> , 850(2), 200 (8pp). doi: 10.3847/1538-4357/aa974e
Type of publication	Article (peer-reviewed)
Link to publisher's version	http://iopscience.iop.org/article/10.3847/1538-4357/aa974e/meta http://dx.doi.org/10.3847/1538-4357/aa974e Access to the full text of the published version may require a subscription.
Rights	© 2017, The American Astronomical Society. All rights reserved.
Item downloaded from	http://hdl.handle.net/10468/6877

Downloaded on 2018-09-30T19:28:14Z



UCC

University College Cork, Ireland
Coláiste na hOllscoile Corcaigh



Constraining Magnetization of Gamma-Ray Bursts Outflows Using Prompt Emission Fluence

Asaf Pe'er 

Physics Department, University College Cork, Cork, Ireland

Received 2016 April 21; revised 2017 October 25; accepted 2017 October 26; published 2017 December 4

Abstract

Considered here is the acceleration and heating of relativistic outflow by local magnetic energy dissipation process in Poynting-flux dominated outflow. Adopting the standard assumption that the reconnection rate scales with the Alfvén speed, I show here that the fraction of energy dissipated as thermal photons cannot exceed $(13\hat{\gamma} - 14)^{-1} = 30\%$ (for adiabatic index $\hat{\gamma} = 4/3$) of the kinetic energy at the photosphere. Even in the most radiatively efficient scenario, the energy released as non-thermal photons during the prompt phase is at most equal to the kinetic energy of the outflow. These results imply that calorimetry of the kinetic energy that can be done during the afterglow phase could be used to constrain the magnetization of gamma-ray bursts (GRB) outflows. I discuss the recent observational status and its implications on constraining the magnetization in GRB outflows.

Key words: (Stars:) Gamma-ray burst: general – magnetic reconnection – magnetohydrodynamics (MHD) – plasmas – radiation mechanisms: non-thermal – radiation mechanisms: thermal

1. Introduction

One of the key open questions in the study of relativistic outflows is the mechanism responsible for accelerating the plasma to ultra-relativistic speeds, with inferred Lorentz factor $\Gamma \gtrsim$ few tens in active galactic nuclei (AGNs) and $\Gamma \gtrsim 100$ in gamma-ray bursts (GRBs). In the classical GRB “fireball” model, for example, the outflow is accelerated by radiative pressure and magnetic fields are sub-dominant (for several recent reviews, see Meszaros & Rees 2014; Kumar & Zhang 2015; Pe'er 2015, and references therein). On the other hand, in recent years, models in which GRB outflows are Poynting-flux dominated became increasingly popular (Levinson 2006; Lyutikov 2006; Giannios 2008; Tchekhovskoy et al. 2008; Komissarov et al. 2009; Metzger et al. 2011; Zhang & Yan 2011; McKinney & Uzdensky 2012; Sironi et al. 2015).

There are indeed strong theoretical arguments in favor of Poynting-flux dominated flows in GRBs. First, it is well established that the progenitor of a GRB is a compact object of solar scale, namely a black hole or neutron star. A Poynting-flux dominated outflow will naturally occur if the compact object rotates and possesses a magnetic field (Blandford & Znajek 1977; Blandford & Payne 1982). The jet could tap into the rotational energy of the neutron star, black hole, or accretion disk through the agency of an ordered magnetic field that threads the source (e.g., Usov 1992; Thompson 1994; Vlahakis & Königl 2001; Drenkhahn 2002; Drenkhahn & Spruit 2002; Lyutikov & Blandford 2003; Vlahakis & Königl 2003). Second, a well-known problem of non-magnetized outflow models is the very low efficiency in converting the kinetic energy to the observed radiation. This must follow an episode(s) of kinetic energy dissipation. However, the leading dissipation mechanism, namely internal shock waves (Rees & Meszaros 1994), are known to be inefficient; typically, only a few % of the kinetic energy is dissipated (Mochkovitch et al. 1995; Kobayashi et al. 1997; Panaitescu et al. 1999). In Poynting-flux dominated flows, on the other hand, dissipation of magnetic energy can take place via a reconnection process. This process is known to provide an efficient way of converting the energy stored in the magnetic

field (Drenkhahn 2002; Drenkhahn & Spruit 2002; Komissarov et al. 2009; Lyubarsky 2010; Tchekhovskoy et al. 2010; McKinney & Uzdensky 2012; Sironi et al. 2015).

The dissipated magnetic energy is converted into (1) kinetic energy of the bulk outflow motion and (2) thermal energy of the outflow. As was long thought and recently proved numerically (Sironi & Spitkovsky 2014; Uzdensky & Spitkovsky 2014), part of the dissipated energy is used to accelerate particles to non-thermal distribution, rather than to heat a thermal distribution of particles to a higher temperature. In the context of energy transfer from the magnetic field, this energy is part of the thermal energy given to the plasma (rather than the kinetic energy). The difference between thermal and non-thermal heating would be manifested in the rate at which this energy could be radiated away. One generally expects that non-thermal particles would radiatively lose their energy faster.

In the context of GRBs, if indeed cooling is efficient, (most of) the thermal energy will be radiated away during the prompt phase, either as thermal photons at the photosphere or as non-thermal photons above it. As opposed to that, the bulk kinetic energy could not be converted into radiation on the short timescale characterizing the prompt phase. Instead, it will gradually dissipate during the afterglow phase. Thus, measurements of the thermal and non-thermal energies during the prompt phase and comparing them to the outflow kinetic energy (that could be deduced from afterglow measurements) would put strong constraints on the validity of the magnetized model.

In this paper, I show that the maximum ratio of thermal to kinetic energy is, in fact, universal and independent of many of the model’s parameters. If radiative cooling is slow, the amount of energy that can be released as thermal photons cannot exceed $(13\hat{\gamma} - 14)^{-1} = 30\%$ (for adiabatic index $\hat{\gamma} = 4/3$) of the kinetic energy. This energy would be released at the photosphere, and will therefore be observed as a (modified) thermal component. I should stress that 30% is an absolute upper limit; as the photospheric radius is expected to be below the saturation radius (namely, occur while the flow still accelerates), only the thermal energy released up until this

radius could be radiated as such. One therefore expects the observed ratio of thermal to kinetic energy to be no more than a few %. On the other extreme, if radiative cooling is efficient, the fraction of energy released as (non-thermal) photons is equal at most to the remaining kinetic energy, regardless of the unknown model parameters, such as the magnetization or the reconnection rate. This implies that within the context of Poynting-flux dominated outflow, the overall radiation observed during the prompt phase cannot exceed the kinetic energy inferred from afterglow observations. Thus, additional—or different—mechanisms must be operating in those GRBs in which the energy released during the prompt phase exceeds the kinetic energy. The obtained results are aligned, of course, with the numerical results obtained in Drenkhahn & Spruit (2002); however, they generalize the numerical results obtained there by providing robust, model-independent upper limits that can be directly compared with observations.

This paper is organized as follows. Section 2 provides the underlying model assumptions. I then calculate the ratio of thermal to kinetic energy released for the slow cooling and fast cooling scenarios in Section 3. Section 4 discusses the current observational status of the prompt and afterglow GRB measurements, as had been accumulated in the past decade or so. I point to gaps in the analysis that could lead to breakthrough in understanding the magnetization in GRBs. Finally, Section 5 discusses the implications and limitations of the Poynting-flux dominated model in view of the existing data before summarizing.

2. Basic Model Assumptions

As a model of Poynting-flux dominated flow, I adopt the “striped wind” model of Coroniti (1990), whose dynamics were studied by several authors (Drenkhahn 2002; Drenkhahn & Spruit 2002; Giannios 2005; Giannios & Spruit 2005; Mészáros & Rees 2011). The magnetic field in the flow changes polarity on a small scale λ , due to rotation of an inclined magnetic dipole. This scale is of the order of the light cylinder in the central engine frame ($\lambda \approx 2\pi c/\Omega$, where Ω is the angular frequency of the central engine: presumably a spinning black hole). The polarity change leads to magnetic dissipation via reconnection process, which is assumed to occur at a constant rate along the jet. As a consequence, the magnetic field decays during a characteristic (comoving) timescale $\tau' = \lambda'/\epsilon v'_A$, where $v'_A \approx c$ is the comoving Alfvénic speed and $\lambda' = \Gamma\lambda$, where Γ is the Lorentz factor of the flow. All the uncertainty in the microphysics of the reconnection process is taken up by the dimensionless factor ϵ , which is often assumed in the literature a fixed value, $\epsilon = 0.1$.

Way above the Alfvénic radius (the radius in which the flow velocity is equal to the Alfvén speed), the flow is assumed to be purely radial. The dominant magnetic field component is $B = B_\phi \gg B_r, B_\theta$. For stationary case in ideal magnetohydrodynamics (MHD), this implies that $\partial_r(\beta rB) = 0$, where β is the outflow velocity, and B is the magnetic field in the observer’s frame. For non-ideal MHD, the evolution of the magnetic field is given by (Drenkhahn 2002; Drenkhahn & Spruit 2002)

$$\partial_r(rub) = -\frac{rb}{c\tau'} = -\frac{rb}{c} \frac{\epsilon\Omega}{2\pi\Gamma}, \quad (1)$$

where $b = B/\sqrt{4\pi}\Gamma$ is the (normalized) magnetic field in the comoving frame, $u = \Gamma\beta$ and $\beta = (1 - \Gamma^{-2})^{1/2}$ is the normalized outflow velocity.

Drenkhahn (2002) showed that for Poynting-flux dominated flow with $\Gamma \gg 1$, the flow accelerates as $\Gamma(r) \propto r^{1/3}$. For the purpose of this work, I point out that this is a very robust result that is independent of the reconnection rate ($\epsilon\Omega$) and can be derived directly from Equation (1), as long as the outflow is Poynting-flux dominated, $L_{\text{pf}} = \Gamma u r^2 b^2 \gg L_k$.

This result can be understood by noting the following. First, for $\Gamma \gg 1$, Equation (1) can be written as $\partial_r(L_{\text{pf}}) \simeq \partial_r(r^2\Gamma^2b^2) \propto -(rb)^2$. Using $L = L_{\text{pf}} + L_k$, conservation of energy implies $\partial_r(L_k) = -\partial_r(L_{\text{pf}}) \propto (rb)^2$. Second, the flux of kinetic energy can be written as $L_k = \dot{M}\Gamma c^2$, where \dot{M} is the mass ejection rate per time per sterad, which is assumed steady. Thus, $\partial_r(L_k) \propto \partial_r(\Gamma)$. Combined together, one obtains $\partial_r\Gamma \propto (rb)^2$. Now, using the assumption $L_{\text{pf}} \gg L_k$, one finds that $L \simeq L_{\text{pf}} = \Gamma^2 r^2 b^2$ which implies $\Gamma^2 \partial_r\Gamma \approx \text{Const}$, with the solution $\Gamma(r) \propto r^{1/3}$.

Dynamic equations. The evolution of the proper mass density, ρ , energy density (excluding rest mass), e , the four-velocity u and the magnetic field strength, b are determined by conservation of mass, energy, and momentum, together with Equation (1). These are combined with the equation of state, $p = (\hat{\gamma} - 1)e$, where $\hat{\gamma}$ is the adiabatic index. When radiative losses are included, these equations take the form (Drenkhahn & Spruit 2002)

$$\partial_r(r^2\rho u) = 0 \rightarrow \dot{M} = r^2\rho u c, \quad (2)$$

$$\partial_r[r^2\Gamma u(\omega + b^2)] = -r^2\Gamma \frac{\Lambda}{c}, \quad (3)$$

$$\partial_r \left[r^2 \left\{ (\omega + b^2)u^2 + \frac{b^2}{2} + p \right\} \right] = 2rp - r^2u \frac{\Lambda}{c}. \quad (4)$$

Here, $\omega = e + p + \rho c^2 = \hat{\gamma}e + \rho c^2$ is the proper enthalpy density, and Λ is the (comoving) emissivity (energy radiated per unit time per unit volume), which is assumed isotropic in the comoving frame.

As the heated particles radiate their energy they cool. The emissivity takes the form

$$\Lambda = k \frac{e c u}{r}, \quad (5)$$

where k is an adjustable cooling length. In Drenkhahn & Spruit (2002), a value of $k = 0$ was taken below the photosphere, justified by the fact that in this regime the photons are coupled to the particles, while $k = 10^4$ was assumed above the photosphere. This high value was justified by the assumption of synchrotron cooling of very energetic particles in the strong magnetic field expected in this scenario. While it is far from being clear that the electrons can be accelerated to very large Lorentz factors in this model (See Bégué et al. 2017), as shown here, in fact the exact value of k is of no importance, as long as $k \gtrsim 1$.

Before solving these equations, we note that for $k = 0$, the energy Equation (3) can be integrated to obtain $L = L_{\text{pf}} + L_k + L_{\text{th}}$, where $L_k (= \dot{M}\Gamma c^2) = r^2\Gamma u c \rho c^2$ is the kinetic luminosity (per steradian) and $L_{\text{th}} = r^2\Gamma u c \hat{\gamma}e$ is the thermal luminosity (per steradian). The thermal luminosity though includes a pressure term, therefore the available luminosity that would be observed if the thermal energy could be entirely released (e.g., at the photosphere) is $L_{\text{th}}^{\text{ob.}} = r^2\Gamma u c e$. When

radiative losses are included ($k > 0$), one can further define a non-thermal luminosity by $L_{\text{NT}} = L - L_{\text{pf}} - L_{\text{th}} - L_k$.

3. Upper Limits on the Ratio of Radiated to Kinetic Energy

The set of Equations (1)–(4) can be simplified for the case $\Gamma \gg 1$, by noting that one can approximate $\Gamma u \simeq u^2 + 1/2$. Using this in the energy Equation (3) and plugging the result in the momentum Equation (4), one obtains

$$\partial_r \left[r^2 \left(p - \frac{\omega}{2} \right) \right] \simeq 2rp + k \frac{re}{2}. \quad (6)$$

This equation implies scaling laws on the energy and number densities, $e = e_0 r^{-7/3}$ and $\rho = \rho_0 r^{-7/3}$.

Slow cooling scenario. Let us first consider the case in which $k = 0$, namely radiative losses are dynamically unimportant. Using $\omega = \hat{\gamma}e + \rho c^2$, $p = (\hat{\gamma} - 1)e$ and the scaling laws obtained above in Equation (6), this equation becomes $\rho_0 c^2 = (13\hat{\gamma} - 14)e_0$, or

$$\frac{L_{\text{th}}^{\text{ob}}}{L_k} = \frac{e_0}{\rho_0 c^2} = \frac{1}{13\hat{\gamma} - 14} = \frac{3}{10}, \quad (7)$$

where the last equality holds for $\hat{\gamma} = 4/3$ (for $\hat{\gamma} = 5/3$, one finds $e_0/\rho_0 c^2 = 3/23$). I stress that this is an absolute upper limit that can be obtained only if the photospheric radius is above the saturation radius (this depends on the reconnection rate). Typically, this is not the case, and the ratio $L_{\text{th}}^{\text{ob}}/L_k$ is significantly less than that obtained in Equation (7).

Fast cooling scenario. From Equation (6), it is clear that for $k \gg 4(\hat{\gamma} - 1) \simeq 1$, the second term in the right-hand side always dominates the first term. The scaling laws for e and ρ are not changed, implying that Equation (6) takes the form

$$\left(1 - \frac{\hat{\gamma}}{2} \right) e_0 + \frac{\rho_0 c^2}{2} = \frac{3}{2} k e_0, \quad (8)$$

or (for $k \gg 1$)

$$\frac{L_{\text{th}}^{\text{ob}}}{L_k} = \frac{e_0}{\rho_0 c^2} \simeq \frac{1}{3k}. \quad (9)$$

One therefore concludes that for $k \gg 1$, the observed thermal luminosity, $L_{\text{th}}^{\text{ob}}$ can be neglected with respect to the kinetic luminosity, L_k .

Using the result $ke = \rho c^2/3$ and neglecting L_{th} relative to L_k and L_{pf} , the energy Equation (3) takes the form

$$\partial_r (L_k + L_{\text{pf}}) = -\frac{L_k}{3r}. \quad (10)$$

As $L_{\text{NT}} \simeq L - L_{\text{pf}} - L_k$, and L is constant, Equation (10) can be written as

$$\partial_r (L_{\text{NT}}) = \frac{L_k}{3r}. \quad (11)$$

During the acceleration episode, in the regime where $\Gamma \gg 1$ the kinetic luminosity scales as $L_k \propto r^{1/3}$ (this result is immediately obtained from the scaling laws of ρ and Γ). Equation (11), therefore, implies both a similar scaling law of $L_{\text{NT}} \propto r^{1/3}$ and a similar scaling coefficient. This means that at the end of the acceleration, $L_{\text{NT}} = L_k$, namely up to one-half of the dissipated magnetic energy could be radiated away, while the other half

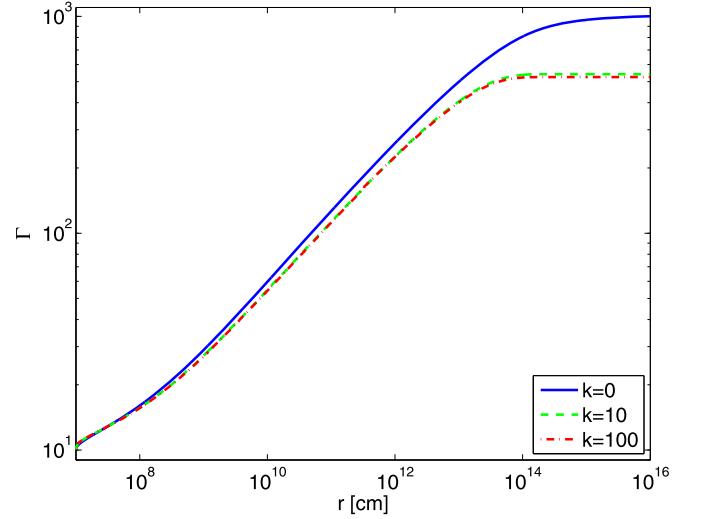


Figure 1. Evolution of the bulk Lorentz factor.

remains in the form of kinetic energy. Further, note that this result is very robust and is independent of any of the unknown model parameters, neither on the adiabatic index. It holds for any value of $k \gg 1$. Similar to the thermal emission calculation, this is an upper limit, which depends on the assumption of strong emissivity along the jet. In reality, all emission mechanisms (synchrotron, Compton, Bremsstrahlung, etc.) will decay with radius, making the observed non-thermal energy to be less than the kinetic energy (Bégué & Pe'er 2015; Bégué et al. 2017).

To demonstrate the validity of the analytical approximations used in deriving these conclusions, I have solved numerically the exact set of Equations (1)–(4) to find the radial evolution of the dynamical variables (Γ , e , ρ and b) and the derived variables (such as L_{pf} , L_k , L_{th} , L_{NT} and u). These set of equations are coupled and stiff; thus, to solve them, I first rewrote them in terms of a variable $\vec{A} = \{L_{\text{pf}}, L_k, L_{\text{th}}, u\}$, and then calculated $d \log(\vec{A})/d \log(r)$. When formulated in this way, standard numerical ordinary differential equation solver could be used.

The results of the numerical calculations are shown in Figures 1–3. In producing the results, I chose as initial conditions $L = 10^{52} \text{ erg s}^{-1} \text{ sterad}^{-1}$, initial magnetization parameter $\sigma_0 \equiv L_{\text{pf},0}/L_{k,0} = 100$ at $r_0 = 10^7 \text{ cm}$ (corresponding to an initial four-velocity $u_0 = \sqrt{\sigma_0} = 10$), and reconnection rate $\epsilon \Omega = 10^3 \text{ s}^{-1}$. The flow was assumed initially cold ($e_0 \equiv e|_{r_0} = 0$), and adiabatic index $\hat{\gamma} = 4/3$ assumed (this is relevant below the photosphere). I chose three different values of $k = 0, 10, 100$ representing possible different emissivities.

Figure 1 presents the evolution of the bulk Lorentz factor. For $k = 0$ case, the outflow terminates at $\Gamma \simeq \sigma_0^{3/2} = 1000$, as predicted by Drenkhahn (2002). In the radiative scenarios, the terminal Lorentz factor is slightly above half of that value (540 and 525 for the $k = 10, 100$ scenarios, respectively), in accordance with the finding that slightly over half of the final energy is in kinetic form.

Figure 2 shows the radial evolution of the various luminosities: L_{pf} , L_k , L_{th} , and L_{NT} for the $k = 0$ and $k = 10$

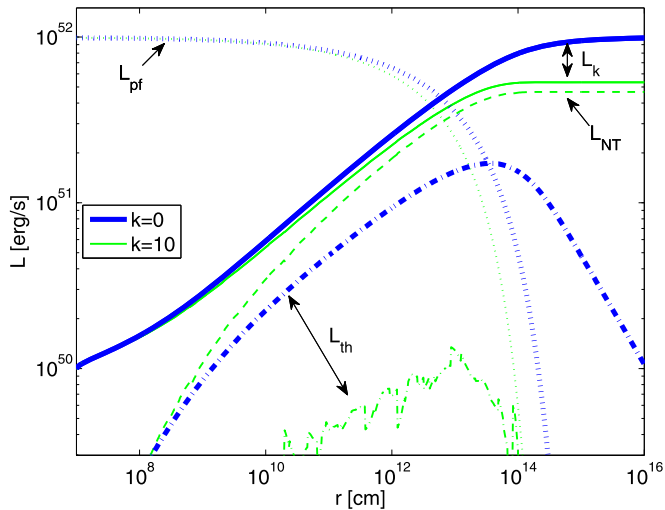


Figure 2. Radial evolution of the luminosities. Thick blue curves are for $k = 0$ scenario, while thin green curves are for the radiative case with $k = 10$. Solid: L_k , dotted: L_{pf} , dashed-dotted: L_{th} , and dashed: L_{NT} . As explained in the text, for large k , the magnetic energy is equally distributed between kinetic and radiated energy, thus L_{NT} approaches L_k .

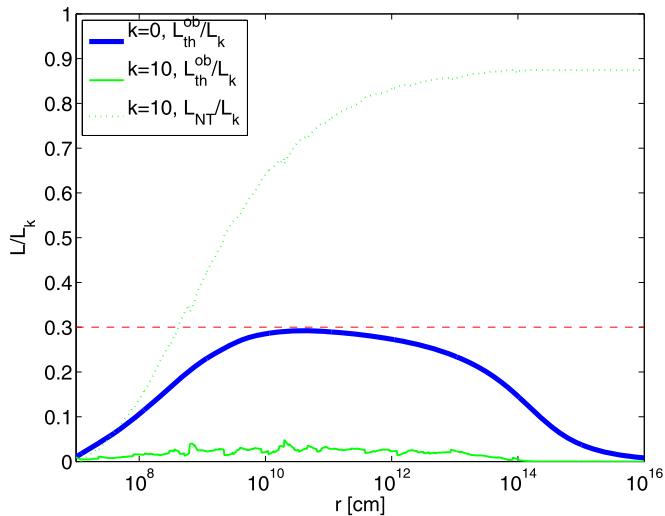


Figure 3. Ratio of observed to kinetic luminosities. Thick blue: $k = 0$ scenario. $L_{th}^{ob}/L_k = 0.3$ (for adiabatic index $\hat{\gamma} = 4/3$). Thin green: $k = 10$. The non-thermal radiated energy reaches slightly less than 90% of the kinetic energy, while the thermal energy is negligible in this scenario.

scenarios (the results obtained for $k = 100$ are very similar to the ones obtained for $k = 10$, thus they are omitted for clarity). All the numerical results are in accordance with the analytical calculations presented above. In particular, when non-thermal radiation is omitted ($k = 0$), the ratio between L_{th} and L_k approaches 30%. This is directly seen in Figure 3. In the radiative scenario ($k = 10$), this ratio is much lower; on the other hand, L_{NT} approaches L_k , as is seen in Figures 2 and 3.

4. Observational Constraints

The results derived above provide two clear predictions about the upper limits of thermal and non-thermal luminosities that can be expected during the prompt emission phase in GRBs. These can be tested with current and future observations, which can therefore be used to test the validity of this model. Identification and analysis of the properties of a thermal

component in GRBs is a relatively new field and, as a result, only sparse data exists to date (see further discussion below). On the other hand, calorimetry of the total radiative efficiency, namely the non-thermal emission of the prompt phase, has been carried out extensively in the past two decades since the discovery of GRB afterglow. It is therefore useful in the context of this work to briefly summarize the existing observational status.

It is common to define the efficiency of the prompt emission radiation as the ratio of the total energy released in gamma-rays (thermal plus non-thermal), divided by the the total (radiative plus kinetic) energy,

$$\eta \equiv \frac{E_\gamma}{(E_k + E_\gamma)}. \quad (12)$$

Within the limits of the observed spectral band, the GRB prompt emission provides a direct probe of the energy released during the prompt phase. The kinetic energy, on the other hand, is estimated by fitting the afterglow observations, which, for historical reasons, are typically available at 11 hr in the X-ray band. The fitting is done within the framework of the ‘‘classical’’ synchrotron model under the assumption that electrons accelerated to a power-law distribution in the propagating forward shock wave. The advantage is that at this time, the reverse shock should already disappear, and the temporal and spectral evolution of the emitted signal should be well characterized by simple scaling laws (Blandford & McKee 1976; Meszaros et al. 1993; Meszaros & Rees 1997; Sari et al. 1998; van Paradijs et al. 2000; Granot & Sari 2002), thereby enabling a reasonably accurate estimate of the outflow kinetic energy.

Few early works that estimated the efficiency of various samples of bursts were carried by Kumar (2000), Freedman & Waxman (2001), Panaitescu & Kumar (2002), Yost et al. (2003), Lloyd-Ronning & Zhang (2004), Zhang et al. (2007), Racusin et al. (2011), D’Avanzo et al. (2012). More recent works not only estimated by efficiency but further the absolute released energy by correcting for the finite jet opening angle (Cenko et al. 2010, 2011; Troja et al. 2012; Guidorzi et al. 2014; Laskar et al. 2014, 2015, 2016). The different samples consist of bursts observed by different instruments thereby having different spectral coverage and used several different methods in estimating the efficiencies. It is therefore impossible to combine all the collected data into one big sample.

Despite these differences, it is very interesting that all these works arrive at the same conclusion, namely that the efficiency varies widely between different bursts within the same sample. It is consistently found that the efficiency is ranging from less than 1% to over 90%, with about one-half of the GRBs in each sample showing efficiency of over 50%. Note that in the notation used in this paper, radiative efficiency of $\eta > 50\%$ is equivalent to $L_{NT} > L_k$, and is thus forbidden within the framework of the Poynting-flux dominated model. As a concrete example, in the analysis carried by Laskar et al. (2015), 13/24 GRBs show $E_\gamma > E_k$, with 11/24 being more than 1σ away from $E_\gamma \leq E_k$. This result is not unique, but is rather representative of all other analyses mentioned above. Interestingly, a similar conclusion was reached when analyzing a large sample of short GRBs (Fong et al. 2015), implying that

the large range of radiative efficiencies appear in both the long and short GRB populations.

This large range of efficiencies found is challenging to all theoretical models, which need to explain both the very high efficiency seen in tens of % of the GRB population, as well as the wide separation between the bursts. Motivated by this challenge, a different analysis method was proposed by Beniamini et al. (2015, 2016). In these works, the authors argue that the late time X-ray flux may not be a good proxy to the kinetic energy, due to either significant synchrotron self Compton radiation that lowers the synchrotron flux at the observed band, or alternatively, a weaker than expected magnetic field that prevents an efficient radiation at the X-ray band (“slow cooling”). Instead, they propose to use the GeV emission seen at much earlier times (hundreds of seconds, though later than the observed time of photons at lower energies) in several LAT-detected GRBs as a better proxy to the remaining kinetic energy.

Using the GeV photons to estimate the kinetic energy results in significantly higher kinetic energy than that inferred from the X-rays and corresponding lower efficiency, which is found to be around 15%. While this model seem to overcome the high-efficiency problem, the use of the GeV emission as a proxy to the kinetic energy needs to be done with great care. First, the inferred energy is much higher (up to two orders of magnitude) than the typical energies inferred at very late times (Shivvers & Berger 2011). Second, it is far from being clear that the GeV photons have synchrotron (rather than inverse Compton) origin, as is assumed in these fits. Third, it is not obvious that the GeV photons originate from the forward shock. On the contrary, it was shown by Pe'er & Waxman (2005) that a significant fraction of the GeV photons expected at this time of hundreds of seconds originate from the reverse shock that could well exist at this epoch, and are upscattered by electrons at the forward shock. Finally, a detailed analysis (B. Gompertz et al. 2017, in preparation) shows that about half of the LAT bursts in the sample used by Beniamini et al. (2015) are in fact in the fast cooling regime.

Nonetheless, the high efficiency inferred by many authors is a major challenge not only to the magnetized model presented here, but to the alternative “internal shocks” model as well. There is broad agreement that the radiative efficiency expected in the internal shock model is not likely to exceed a few percent to a few tens of percent at most (Kobayashi et al. 1997; Daigne & Mochkovitch 1998; Guetta et al. 2001; Ioka et al. 2006; Pe'er et al. 2017), though it was shown that under extreme conditions, higher efficiency could be reached in this model (e.g., Beloborodov 2000; Kobayashi & Sari 2001).

There are two important possible caveats of the efficiency estimates presented in the literature to date, which are related to estimate of the kinetic energy, E_k from afterglow data. The first is that many of the above-mentioned works assume a “top hat” jet; namely, they neglect any internal jet structure of the form $\Gamma = \Gamma(\theta)$ (Γ is the jet Lorentz factor and the angle θ is measured from the jet axis). On the other hand, simple phase-space argument implies that in most observed GRBs the observer is located off the jet axis. While the structure of the jets are unknown, angle-dependent Lorentz factor could lead to an uncertainty in the estimated value of the kinetic energy by a factor of up to a few.

A second caveat relates to the microphysics of particle acceleration. Despite major progress in recent years in

understanding particle acceleration in shock waves, the fraction of electrons accelerated to high energies in relativistic shocks is still uncertain. As was pointed out by Eichler & Waxman (2005), there is a degeneracy in interpreting the observed afterglow signal between the fraction of particles accelerated (and emitting the radiation), the jet kinetic energy as well as other parameters such as the density and the magnetic field. Thus, it is possible to explain the observed signal in a model in which a relatively small fraction of electrons are accelerated, provided that the kinetic energy is high, which will reflect in a lower efficiency than estimated by the works discussed above.

While these caveats put strong constraints on the ability of current models to accurately estimate the prompt phase efficiency, in recent years there is a major progress in modeling structured jets observed off-axis (e.g., Zhang & MacFadyen 2009; van Eerten & MacFadyen 2012, 2013), which enable to break some of the degeneracy involved in the jet structure and viewing angle (Ryan et al. 2015). Similarly, advances in numerical, particle-in-cell simulations enabled much better understanding of the microphysics of particle acceleration (Spitkovsky 2008; Sironi & Spitkovsky 2011), which could be used to constrain the fractions of non-thermal and thermal particles heated by the external shock (Giannios & Spitkovsky 2009). It is thus anticipated that much better observational constraints on the efficiency will become available in the near future.

A second prediction of the magnetized model presented here is an upper limit on the ratio of the released thermal energy to kinetic energy. In recent years, it became evident that thermal emission component does exist in several bright GRBs, such as GRB090902B (Abdo et al. 2009; Ryde et al. 2011), GRB100724B (Guiriec et al. 2011), GRB090510 (Ackermann et al. 2010), GRB110721A (Axelsson et al. 2012; Iyyani et al. 2013), GRB110920A (Iyyani et al. 2015) and others. In a few bright GRBs, such as GRB090902B, it clearly dominated the spectrum.

However, no systematic analysis was carried so far about the relative strength and ubiquitousness of the thermal component. Partially, this is due to the fact that a firm detection of a thermal component is relatively difficult, as (1) it requires a different template than the commonly used “Band” function fit, and (2) there are various effects that act to smear (broaden) the signal; see Pe'er & Ryde (2017) for details. Despite this, there is an increasing evidence that a thermal component is more ubiquitous among bright GRBs (F. Ryde et al. 2017, in preparation). This can be understood, as a clear detection of a thermal component requires a more refined template in fitting the observed spectrum. It is therefore more difficult to detect in weak GRBs, in which the number of photons are limited. If confirmed, this result therefore suggests that a thermal component might in fact be very ubiquitous; in many GRBs in which it is not detected, it is mainly due to technical reasons, as, due to their cosmological distribution and the detectors limitations, most GRBs are detected close to the detector’s limit. The results presented here thus raise the need for a more comprehensive analysis of both the thermal and the non-thermal flux as a key way in constraining the outflow magnetization.

5. Implications and Limitations

The energy released as thermal and non-thermal during the acceleration phase (L_{th} and L_{NT}) would be directly observed during the prompt phase, either as thermal photons released at

the photosphere or as non-thermal photons released at larger radii. As opposed to that, the kinetic energy (L_k) could not be directly observed during the prompt phase, unless an additional, non-magnetized dissipation process takes place. Such a process might be shock waves, that could develop as a result of instabilities in the flow. In particular, these might be expected at large radii, where the magnetization is weak; this phenomenon is discussed below. However, as pointed in the literature, substantial kinetic energy released by collisions is generally less favorable due to the low efficiency of this process.

Instead, the kinetic energy will be gradually released during the afterglow phase; it will be used to accelerate and heat particles from the ambient medium, which will radiate the observed afterglow. As discussed in Section 4, the very high efficiency of radiation during the prompt phase, if indeed confirmed, challenges the validity of the magnetized model.

This difficulty adds to the difficulty of magnetized models to account for a significant, sub-MeV thermal component (Zhang & Pe'er 2009; Bégué & Pe'er 2015) as is reported in several bursts. Interestingly, very similar results are obtained within the reconnection model suggested by Lyubarsky & Kirk (2001), in which different assumptions about the reconnection rate lead to different scaling law $\Gamma \propto r^{1/2}$.

One possible solution within the framework of Poynting-flux dominated flows is to invoke a more complicated dissipation scheme. For example, one may assume that the dissipation of the magnetic energy does not occur continuously along the jet, but only in specific regions. This could be triggered, e.g., by outflow discontinuities such as turbulence (e.g., Zhang & Yan 2011). However, detailed numerical models carried out so far of more complicated outflow dynamics (Deng et al. 2015) did not reveal a substantially different dynamics than the simple 1D model analyzed in this work, nor better efficiency than derived here. Another possibility is Compton drag (namely, the emitted radiation is non-isotropic in the comoving frame). In this scenario, somewhat higher efficiency could be achieved under the appropriate conditions (Levinson & Globus 2016).

A detailed model by McKinney & Uzdensky (2012) suggested that the rate of reconnection changes along the jet, from being slow (Sweet–Parker like geometry) at small radii to fast (Petschek-like geometry) at larger radii. This transition is initiated by a change in the plasma conditions, from being collisional to collisionless. The transition could occur if certain conditions are met, such as the production of a large number of pairs in the inner jet regions that later annihilate at large radii. Despite the different underlying assumptions, McKinney & Uzdensky (2012) find that the outflow dynamics in this scenario is not substantially different than the one considered here. The main application of this scenario would therefore be a reduction of the relative strength of the thermal component, as most of the dissipation occurs above the photosphere.

The simplified dynamics considered here may be modified by variations in the conditions at the base of the jet. Such fluctuations could lead to internal shocks, which would further dissipate part of the kinetic energy and thereby increase the efficiency of the prompt emission beyond the values calculated here. This is due to the fact that additional source of energy (associated with the relative motion of the outflow) is added to the energy associated with the dissipation of the magnetic field.

In general, internal shocks are expected in region of low magnetization, namely $\sigma < 1$. While the focus in this work is on highly magnetized flows, as shown in Section 3, due to the dissipation of the magnetic energy that is used to accelerate the flow, at sufficiently large radii the magnetic energy becomes sub-dominant (see Figure 2). Furthermore, in a scenario of variable, magnetized outflow, magnetic energy conversion inside a plasma shell may occur directly as a result of magnetic pressure within a shell (Granot et al. 2011). These internal shocks can dissipate a substantial fraction of the differential kinetic energy between the shells, in both the low-magnetic as well as in magnetized shell scenarios (Granot 2012).

A detailed calculation of the modification of the efficiency calculated here due to internal shocks is beyond the scope of this work. This is due to the fact that in this scenario, the efficiency of kinetic energy conversion depends on the configuration of the magnetic fields, as well as the initial conditions at the jet base. Several works that dealt with strong toroidal field concluded that the efficiency is not expected to be high, typically a few percent at most for magnetization parameter $\sigma \geq 10$ (Kennel & Coroniti 1984; Zhang & Kobayashi 2005; Narayan et al. 2011; Komissarov 2012). It is found in these works that there is an inverse correlation: a stronger magnetization leads to a lower efficiency in energy conversion by shock waves.

Furthermore, if the magnetic field have a strong poloidal component, the formation of shock waves is suppressed, and it is not clear that the shock waves could be formed at all (Bret et al. 2017). These results therefore suggest that the efficiency derived here might not be heavily modified in the presence of internal shocks if they occur in a regime dominated by poloidal field.

Alternatively, most of the prompt emission photons may have a different origin. An appealing alternative is emission from the photosphere. Thermal photons may exist in the plasma at early stages and advect with it until the photosphere in which they decouple. Thus, their existence does not require high efficiency in kinetic or magnetic energy conversion. Indeed, there is increasing evidence that a significant thermal component is ubiquitous (e.g., Lazzati et al. 2013, and Section 4 in this paper). In recent years, it was demonstrated that the observed spectrum of photons emerging from the photosphere can deviate substantially from the naively expected “Planck” spectrum. This is due to both light aberration effects (Pe'er 2008; Lundman et al. 2013) as well as possible sub-photospheric energy dissipation (e.g., Pe'er et al. 2006).

6. Summary and Conclusions

This paper considers the “striped wind” model of a Poynting-flux dominated outflow in GRBs, in which the main source of energy is dissipation of magnetic fields. The dissipated magnetic energy is used to both accelerate the outflow and heat particles in the plasma, which then radiate, producing both thermal and non-thermal emission. I derived here simple analytical upper limits on the ratio of thermal to kinetic energy, $L_{th}/L_k = 30\%$ (Equation (7)) and non-thermal to kinetic energy $L_{NT}/L_k = 50\%$ (Equation (11)), and confronted these upper limits with observations in Section 4.

The analytical upper limits and numerical results derived here are aligned with the numerical results obtained by Drenkhahn & Spruit (2002), albeit a larger value of k (very fast cooling) was used in that work. The ratio of thermal to total

kinetic energy was calculated previously only numerically, by Drenkhahn & Spruit (2002), and later on by Giannios & Spruit (2007). These works found that this ratio is at the range of 20%–30% (though a maximum value of 35% was found numerically) for the parameter range considered. The analytical results derived here thus provide a simple explanation to the numerical works. Similarly, the ratio of 50% of non-thermal to kinetic energy was derived numerically by Drenkhahn & Spruit (2002). A heuristic, yet insightful argument for the validity of this result was provided by Spruit & Drenkhahn (2004).¹ The present work thus generalizes previous treatments of the striped wind model scenario by providing analytical arguments that prove the robustness of the upper limits obtained on the ratios of both the thermal and non-thermal fluxes. These limits are independent on uncertainties such as the initial magnetization parameter, magnetic dissipation rate, cooling rate, or adiabatic index.

By now there are ample of works measuring the radiative efficiency of non-thermal GRB prompt emission. Despite the use of different samples and different methods, a repeated result is that the efficiency considerably varies among GRBs within the same sample, with about half the bursts showing efficiency greater than the allowed by the magnetized outflow scenario. As discussed in Section 4, there is a large uncertainty in the estimate of the efficiency due to the unknown jet structure and the microphysics of particle acceleration. This high efficiency is further difficult to explain within the framework of the alternative “internal shocks” model as well. Thus, it calls for a deep re-analysis using both broadband and time-dependent data to validate these results.

A key result of this work is the upper limit on the thermal flux. While it is clear today that a thermal emission component exists in many GRBs, it is still uncertain how ubiquitous it is and how strong it is among different bursts. The analysis carried here thus calls for a re-analysis of GRB prompt emission in order to identify thermal component that could constrain the magnetization. Indeed, as was already pointed out, e.g., by Zhang & Pe'er (2009) and is further strengthened here, identification of a strong thermal component is likely the best observational way of constraining the outflow magnetization.

It is clear that the dynamical model used here is simplified, as it cannot account for variation in the outflow. However, the rate of reconnection depends on the exact configuration of the magnetic field and therefore can only be tracked by numerical MHD models. Existing numerical results (McKinney & Uzdensky 2012) suggest that the outflow dynamics may in fact be close to the simplified model used here. This fact may further be used to constrain the validity of the magnetized model in explaining the dynamics of GRB outflows, in particular in those GRBs in which the light curve is highly variable. It may further suggest a correlation between the observed light curve variability and the existence of a strong thermal component, as both are characterizing outflows which are only weakly magnetized.

A.P. thanks Damien Bogue, Brad Cenko, Amir Levinson, Yuri Lyubarski, Raffaella Margutti, and Bing Zhang for useful comments. I further thank the anonymous referee for useful comments that helped improve this manuscript. This research

was partially supported by the European Union Seventh Framework Programme (FP7/2007-2013) under grant agreement n° 618499. I further acknowledge support from NASA under grant #NNX12AO83G.

ORCID iDs

Asaf Pe'er  <https://orcid.org/0000-0001-8667-0889>

References

- Abdo, A. A., Ackermann, M., Ajello, M., et al. 2009, *ApJL*, 706, L138
 Ackermann, M., Asano, K., Atwood, W. B., et al. 2010, *ApJ*, 716, 1178
 Axelsson, M., Baldini, L., Barbiellini, G., et al. 2012, *ApJL*, 757, L31
 Bégué, D., & Pe'er, A. 2015, *ApJ*, 802, 134
 Bégué, D., Pe'er, A., & Lyubarsky, Y. 2017, *MNRAS*, 467, 2594
 Beloborodov, A. M. 2000, *ApJL*, 539, L25
 Beniamini, P., Nava, L., Duran, R. B., & Piran, T. 2015, *MNRAS*, 454, 1073
 Beniamini, P., Nava, L., & Piran, T. 2016, *MNRAS*, 461, 51
 Blandford, R. D., & McKee, C. F. 1976, *PhFl*, 19, 1130
 Blandford, R. D., & Payne, D. G. 1982, *MNRAS*, 199, 883
 Blandford, R. D., & Znajek, R. L. 1977, *MNRAS*, 179, 433
 Bret, A., Pe'er, A., Sironi, L., Sadowski, A., & Narayan, R. 2017, *JPIPh*, 83, 715830201
 Cenko, S. B., Frail, D. A., Harrison, F. A., et al. 2010, *ApJ*, 711, 641
 Cenko, S. B., Frail, D. A., Harrison, F. A., et al. 2011, *ApJ*, 732, 29
 Coroniti, F. V. 1990, *ApJ*, 349, 538
 Daigne, F., & Mochkovitch, R. 1998, *MNRAS*, 296, 275
 D'Avanzo, P., Salvaterra, R., Sbarufatti, B., et al. 2012, *MNRAS*, 425, 506
 Deng, W., Li, H., Zhang, B., & Li, S. 2015, *ApJ*, 805, 163
 Drenkhahn, G. 2002, *A&A*, 387, 714
 Drenkhahn, G., & Spruit, H. C. 2002, *A&A*, 391, 1141
 Eichler, D., & Waxman, E. 2005, *ApJ*, 627, 861
 Fong, W., Berger, E., Margutti, R., & Zauderer, B. A. 2015, *ApJ*, 815, 102
 Freedman, D. L., & Waxman, E. 2001, *ApJ*, 547, 922
 Giannios, D. 2005, *A&A*, 437, 1007
 Giannios, D. 2008, *A&A*, 480, 305
 Giannios, D., & Spitkovsky, A. 2009, *MNRAS*, 400, 330
 Giannios, D., & Spruit, H. C. 2005, *A&A*, 430, 1
 Giannios, D., & Spruit, H. C. 2007, *A&A*, 469, 1
 Granot, J. 2012, *MNRAS*, 421, 2467
 Granot, J., Komissarov, S. S., & Spitkovsky, A. 2011, *MNRAS*, 411, 1323
 Granot, J., & Sari, R. 2002, *ApJ*, 568, 820
 Guetta, D., Spada, M., & Waxman, E. 2001, *ApJ*, 557, 399
 Guidorzi, C., Mundell, C. G., Harrison, R., et al. 2014, *MNRAS*, 438, 752
 Guirrec, S., Connaughton, V., Briggs, M. S., et al. 2011, *ApJL*, 727, L33
 Ioka, K., Toma, K., Yamazaki, R., & Nakamura, T. 2006, *A&A*, 458, 7
 Iyyani, S., Ryde, F., Ahlgren, B., et al. 2015, *MNRAS*, 450, 1651
 Iyyani, S., Ryde, F., Axelsson, M., et al. 2013, *MNRAS*, 433, 2739
 Kennel, C. F., & Coroniti, F. V. 1984, *ApJ*, 283, 694
 Kobayashi, S., Piran, T., & Sari, R. 1997, *ApJ*, 490, 92
 Kobayashi, S., & Sari, R. 2001, *ApJ*, 551, 934
 Komissarov, S. S. 2012, *MNRAS*, 422, 326
 Komissarov, S. S., Vlahakis, N., Königl, A., & Barkov, M. V. 2009, *MNRAS*, 394, 1182
 Kumar, P. 2000, *ApJL*, 538, L125
 Kumar, P., & Zhang, B. 2015, *PhR*, 561, 1
 Laskar, T., Alexander, K. D., Berger, E., et al. 2016, *ApJ*, 833, 88
 Laskar, T., Berger, E., Margutti, R., et al. 2015, *ApJ*, 814, 1
 Laskar, T., Berger, E., Tanvir, N., et al. 2014, *ApJ*, 781, 1
 Lazzati, D., Morsony, B. J., Margutti, R., & Begelman, M. C. 2013, *ApJ*, 765, 103
 Levinson, A. 2006, *ApJ*, 648, 510
 Levinson, A., & Globus, N. 2016, *MNRAS*, 458, 2269
 Lloyd-Ronning, N. M., & Zhang, B. 2004, *ApJ*, 613, 477
 Lundman, C., Pe'er, A., & Ryde, F. 2013, *MNRAS*, 428, 2430
 Lyubarsky, Y., & Kirk, J. G. 2001, *ApJ*, 547, 437
 Lyubarsky, Y. E. 2010, *MNRAS*, 402, 353
 Lyutikov, M. 2006, *NJPh*, 8, 119
 Lyutikov, M., & Blandford, R. 2003, arXiv:astro-ph/0312347
 McKinney, J. C., & Uzdensky, D. A. 2012, *MNRAS*, 419, 573
 Meszaros, P., Laguna, P., & Rees, M. J. 1993, *ApJ*, 415, 181
 Meszaros, P., & Rees, M. J. 1997, *ApJ*, 476, 232
 Mészáros, P., & Rees, M. J. 2011, *ApJL*, 733, L40
 Meszaros, P., & Rees, M. J. 2014, arXiv:1401.3012

¹ The argument appears in full only in the arXiv version of the proceedings.

- Metzger, B. D., Giannios, D., Thompson, T. A., Bucciantini, N., & Quataert, E. 2011, *MNRAS*, **413**, 2031
- Mochkovitch, R., Maitia, V., & Marques, R. 1995, *Ap&SS*, **231**, 441
- Narayan, R., Kumar, P., & Tchekhovskoy, A. 2011, *MNRAS*, **416**, 2193
- Panaiteescu, A., & Kumar, P. 2002, *ApJ*, **571**, 779
- Panaiteescu, A., Spada, M., & Mészáros, P. 1999, *ApJL*, **522**, L105
- Pe'er, A. 2008, *ApJ*, **682**, 463
- Pe'er, A. 2015, *AdAst*, **2015**, 907321
- Pe'er, A., Long, K., & Casella, P. 2017, *ApJ*, **846**, 54
- Pe'er, A., Mészáros, P., & Rees, M. J. 2006, *ApJ*, **642**, 995
- Pe'er, A., & Ryde, F. 2017, *IJMPD*, **26**, 1730018
- Pe'er, A., & Waxman, E. 2005, *ApJ*, **633**, 1018
- Racusin, J. L., Oates, S. R., Schady, P., et al. 2011, *ApJ*, **738**, 138
- Rees, M. J., & Meszaros, P. 1994, *ApJL*, **430**, L93
- Ryan, G., van Eerten, H., MacFadyen, A., & Zhang, B.-B. 2015, *ApJ*, **799**, 3
- Ryde, F., Pe'er, A., Nymark, T., et al. 2011, *MNRAS*, **415**, 3693
- Sari, R., Piran, T., & Narayan, R. 1998, *ApJL*, **497**, L17
- Shivvers, I., & Berger, E. 2011, *ApJ*, **734**, 58
- Sironi, L., Petropoulou, M., & Giannios, D. 2015, *MNRAS*, **450**, 183
- Sironi, L., & Spitkovsky, A. 2011, *ApJ*, **726**, 75
- Sironi, L., & Spitkovsky, A. 2014, *ApJL*, **783**, L21
- Spitkovsky, A. 2008, *ApJL*, **682**, L5
- Spruit, H. C., & Drenkhahn, G. D. 2004, in ASP Conf. Ser. 312, Gamma-Ray Bursts in the Afterglow Era, ed. M. Feroci et al. (San Francisco, CA: ASP), 357
- Tchekhovskoy, A., McKinney, J. C., & Narayan, R. 2008, *MNRAS*, **388**, 551
- Tchekhovskoy, A., Narayan, R., & McKinney, J. C. 2010, *NewA*, **15**, 749
- Thompson, C. 1994, *MNRAS*, **270**, 480
- Troja, E., Sakamoto, T., Guidorzi, C., et al. 2012, *ApJ*, **761**, 50
- Usov, V. V. 1992, *Natur*, **357**, 472
- Uzdensky, D. A., & Spitkovsky, A. 2014, *ApJ*, **780**, 3
- van Eerten, H., & MacFadyen, A. 2013, *ApJ*, **767**, 141
- van Eerten, H. J., & MacFadyen, A. I. 2012, *ApJL*, **747**, L30
- van Paradijs, J., Kouveliotou, C., & Wijers, R. A. M. J. 2000, *ARA&A*, **38**, 379
- Vlahakis, N., & Königl, A. 2001, *ApJL*, **563**, L129
- Vlahakis, N., & Königl, A. 2003, *ApJ*, **596**, 1080
- Yost, S. A., Harrison, F. A., Sari, R., & Frail, D. A. 2003, *ApJ*, **597**, 459
- Zhang, B., & Kobayashi, S. 2005, *ApJ*, **628**, 315
- Zhang, B., Liang, E., Page, K. L., et al. 2007, *ApJ*, **655**, 989
- Zhang, B., & Pe'er, A. 2009, *ApJL*, **700**, L65
- Zhang, B., & Yan, H. 2011, *ApJ*, **726**, 90
- Zhang, W., & MacFadyen, A. 2009, *ApJ*, **698**, 1261